Role of Protein−Water Interactions and Electrostatics in α-Synuclein Fibril Formation†

Larissa A. Munishkina,§ Jeremy Henriques,§ Vladimir N. Uversky,*,§,‡ and Anthony L. Fink*,§

Department of Chemistry and Biochemistry, University of California, Santa Cruz, California 95064, and Institute for Biological Instrumentation, Russian Academy of Sciences, Pushchino, Moscow Region 142292, Russia

Received June 2, 2003; Revised Manuscript Received January 14, 2004

ABSTRACT: Deposition of misfolded α-synuclein is a critical factor in several neurodegenerative disorders. Filamentous α-synuclein is the major component of Lewy bodies and Lewy neurites, the intracellular inclusions in the dopaminergic neurons of the *substantia nigra*, which are considered the pathological hallmark of Parkinson's disease. We show here that anions induce partial folding of α-synuclein at neutral pH, forming a critical amyloidogenic intermediate, which leads to significant acceleration of the rate of fibrillation. The magnitude of the accelerating effect generally followed the position of the anions in the Hofmeister series, indicating a major role of protein−water−anion interactions in the process at salt concentrations above 10 mM. Below this concentration, electrostatic effects dominated in the mechanism of anion-induced fibrillation. The acceleration of fibrillation by anions was also dependent on the cation. Moderate concentrations of anions affected both the rates of nucleation and the elongation of α-synuclein fibrillation, primarily via their effect on the interaction of the protein with water.

Parkinson's disease (PD)[1] is a slowly progressive disease resulting from loss of dopaminergic neurons in the *substantia nigra* (*1*, *2*). The aggregation of the presynaptic protein, α-synuclein, has been implicated in the formation of Lewy bodies and Lewy neurites, the intracellular inclusions characteristic of PD, and has been implicated in the etiology of the disease. Thus, although the molecular basis for the neurodegeneration in PD and other synucleinopathies is unknown as yet, the accumulation of α-synuclein-derived fibrillar material represents a potential link between protein misfolding and pathogenesis of these disorders.

α-Synuclein is a small (140 amino acid residues), soluble, intracellular, highly conserved protein, of unknown function, that is abundant in various regions of the brain (*3*−*6*) and has been estimated to account for as much as 1% of the total protein in soluble cytosolic brain fractions (*5*). The amino acid sequence of α-synuclein is characterized by six imperfect repeats (consensus KTKEGV) within the N-terminal half of the polypeptide, as well as by a highly acidic carboxyl-terminal region (*6*−*8*). Purified α-synuclein at neutral pH is characterized by a lack of ordered structure; i.e., it belongs to the family of natively unfolded or intrinsically unstructured proteins (*9*). α-Synuclein readily forms fibrils in vitro, with morphology and staining characteristics similar to those of fibrils extracted from disease-affected brain (*9*−*17*). The kinetics of fibrillation are consistent with a nucleation-dependent mechanism (*11*), in which the critical early stage involves the structural transformation into a partially folded intermediate (*9*).

The rate of α-synuclein fibrillation is significantly accelerated by various environmental factors, including low pH and high temperature (*9*), heparin and other GAGs (*18*), metal cations (*19*, *20*), polycations, including spermine, polyethyleneimine, poly-L-lysine, and poly-L-arginine (*21*), low concentrations of TMAO (*22*) simple and fluorinated alcohols (*23*), and certain pesticides (*20*, *24*, *25*). Accelerated fibrillation of α-synuclein in the presence of low concentrations of organic solvents (TMAO and alcohols) was shown to be due to the specific solvent-induced stabilization of an amyloidogenic partially folded intermediate (*22*, *23*). A model has been suggested in which cations and pesticides interact with α-synuclein to bring about a conformational change to a partially folded state with a high propensity to aggregate (*19*, *20*, *24*, *25*). The mechanisms of partially folded intermediate formation were suggested to be different for metal cations and pesticides. As the C-terminal region of α-synuclein (about 40 amino acids) is very rich in acidic residues and thus highly negatively charged at neutral pH, the resulting repulsive interactions are a major factor leading to the natively unfolded conformation of this protein. It has been suggested that the dominant effect of metal ions on α-synuclein conformational change and fibrillation is due to masking of the Coulombic charge−charge repulsion (*19*, *20*). Similarly, polycations accelerate α-synuclein fibrillation by minimizing the electrostatic repulsion between negatively charged α-synuclein molecules, resulting in a high localized concentration of α-synuclein favoring fibrillation (*21*, *26*).

† This research was supported by Grant RO1 NS39985 from the National Institutes of Health.

* To whom correspondence should be addressed. Telephone: (831) 459-2744. Fax: (831) 459-2935. E-mail: uversky@hydrogen.ucsc.edu and fink@chemistry.ucsc.edu.

§ University of California, Santa Cruz.

‡ Russian Academy of Sciences.

[1] Abbreviations: PD, Parkinson's disease; AD, Alzheimer's disease; LB, Lewy bodies; LN, Lewy neuritis; DLB, dementia with LB; LBVAD, LB variant of AD; MSA, multiple-system atrophy; WT, wild type; GAG, glycosaminoglycan; TMAO, trimethylamine-*N*-oxide; CD, circular dichroism; DLS, dynamic light scattering; ThT, thioflavin T; LDW, low-density water.

10.1021/bi034938r CCC: $27.50
Published on Web 02/27/2004

In this study we analyzed the effect of different anions on the structure and fibrillation of this interesting protein. The anions accelerated the rate of both nucleation and elongation/growth of fibrils in a concentration-dependent manner. The effectiveness of different anions in accelerating fibrillation was analyzed in the context of several possible models to account for their effects, namely the Debye−Hückel screening effect, direct interaction with positive charges (specific anion binding), and effects on the interaction of water with anions and protein (Hofmeister series).

MATERIALS AND METHODS

Materials. Thioflavin T was obtained from Sigma (St. Louis, MO). All other chemicals were of analytical grade from Fisher Chemicals or VWR Scientific.

Methods. Purification of α-Synuclein. Human wild-type α-synuclein was expressed in the *Escherichia coli* BL21-(DE3) cell line transfected with pRK172/α-synuclein WT plasmid (kind gift of M. Goedert, MRC Cambridge) and purified as previously described (*27*) with some modifications. Briefly, the pellet from 2 L of cells induced with 0.5 mM isopropyl *β*-D-thiogalactopyranoside was lysed by sonication at 0 °C in 50 mM NaCl, 20 mM Tris-HCl, 0.10% Triton-X100, 0.20 mM phenylmethylsulfonyl fluoride at pH 8.0. The lysis suspension was brought to 30% saturation with ammonium sulfate at 0 °C (pellet discarded), followed by 50% saturation with ammonium sulfate. The resultant pellet was dialyzed against 50 mM NaCl, 20 mM Tris-HCl, pH 7.5, loaded onto a 25 mm × 130 mm DEAE Sepharose fast-flow column (Amersham Pharmacia Biotech) equilibrated in the same buffer, and eluted with a 50−450 mM NaCl gradient. Fractions containing α-synuclein were dialyzed exhaustively against water, clarified by centrifugation, and lyophilized for storage at −20 0 °C. The resultant α-synuclein protein was judged to be >95% pure following SDS−polyacrylamide electrophoresis, gel filtration, and MS analysis. Lyophilized protein was dissolved immediately before use in deionized, purified H_2O, and the pH was adjusted to 10 ± 0.5 with 0.1 N NaOH (about 3 mM final) to solubilize any aggregated protein. After 10 min of incubation at room temperature, the pH was readjusted to 7−8 with 0.1 N HCl. The protein concentration was determined by measuring the absorbance at 275 nm and using an extinction coefficient of 0.40 mg^{-1} cm^2. For fibrillation assays, the solution was centrifuged at 100 000 rpm for 5 min prior to starting the incubation.

Circular Dichroism Measurements. CD spectra were obtained with an AVIV 60DS spectrophotometer (Lakewood, NJ) using α-synuclein concentrations of 0.5 mg/mL. Spectra were recorded in 0.01 cm cells from 250 to 190 nm with a step size of 1.0 nm, a bandwidth of 1.5 nm, and an averaging time of 4 s. For all spectra, an average of eight scans were obtained. CD spectra of the appropriate buffers were recorded and subtracted from the protein spectra.

Analysis of Spectroscopic Data in the Form of Parametric Dependencies. The "phase diagram" method of analyzing spectroscopic data is extremely sensitive for the detection of intermediate states (*23, 28−32*). Although this method was developed for the analysis of fluorescence data, it can be used with any spectroscopic technique. The essence of this method is to build up the diagram of $I(\lambda_1)$ versus $I(\lambda_2)$, where $I(\lambda_1)$ and $I(\lambda_2)$ are the spectral intensity values measured at wavelengths λ_1 and λ_2 under different experimental conditions for a protein undergoing structural transformations (*23, 28−32*).

Thioflavin T Fluorescence Assay To Monitor Fibrillation. Assay solutions contained protein at a concentration of 1.0 mg/mL (70 μM) in 10 mM sodium phosphate, pH 8.4, at room temperature, containing 20 μM ThT with various concentrations of different sodium salts, as indicated. For the low-pH experiments, the pH was 2.0. A volume of 150 μL of the mixture was pipetted into a well of a 96-well plate (white plastic, clear bottom), and a $^1/_8$-in.-diameter Teflon sphere (McMaster-Carr, Los Angeles) was added. We have shown that the kinetics of α-synuclein fibrillation are unaffected by the presence of ThT during incubation under these conditions. Each sample was run in triplicate or quadruplicate. The plates were sealed with Mylar plate sealers (Dynex). The plate was loaded into a fluorescence plate reader (Fluoroskan Ascent) and incubated at 37 °C with shaking at 150 rpm with a shaking diameter of 20 mm. The rate of fibrillation is very sensitive to the shaking speed, and a constant shaking speed was used for all samples within each experiment. The fluorescence was measured at 30 min intervals with excitation at 450 nm and emission at 485 nm, with a sampling time of 100 ms. Data from replicate wells were averaged before plotting fluorescence vs time and fit to an empirical equation (*33*). The standard deviations were usually ∼3% for the rate of fibril elongation and ∼1.5% for the time to half-maximum.

Electron Microscopy. Transmission electron micrographs were collected using a JEOL JEM-100B microscope operating with an accelerating voltage of 80 kV. Typical nominal magnifications were 75 000. Samples were deposited on Formvar-coated 300 mesh copper grids and negatively stained with 1% aqueous uranyl acetate.

RESULTS

Effects of Different Anions on the Structure of α-Synuclein at Neutral pH. We have previously shown that fibril formation of α-synuclein correlates with population of a partially folded intermediate that is characterized by increased secondary structure compared to the normal unfolded conformation of soluble monomeric α-synuclein (*9*). Hence, we initially investigated the effects of both concentration and specific anion on the far-UV circular dichroism of α-synuclein.

Effect of NaCl on the Secondary Structure of α-Synuclein. The influence of increasing NaCl concentration on α-synuclein secondary structure has been analyzed using far-UV CD spectroscopy. Figure 1A shows that, in the absence of NaCl, the spectrum of α-synuclein was typical of an unfolded polypeptide chain, with a minimum in the vicinity of 198 nm and the absence of characteristic bands in the vicinity of 210−230 nm. The addition of as little as 10 mM NaCl significantly increased the content of ordered secondary structure, manifested by a decrease in the minimum at 198 nm accompanied by an increase in negative ellipticity around 222 nm. Interestingly, the shape and the intensity of the far-UV CD spectra did not change much with subsequent increases in NaCl concentration. Overall, the far-UV CD spectrum of α-synuclein in the presence of NaCl was similar

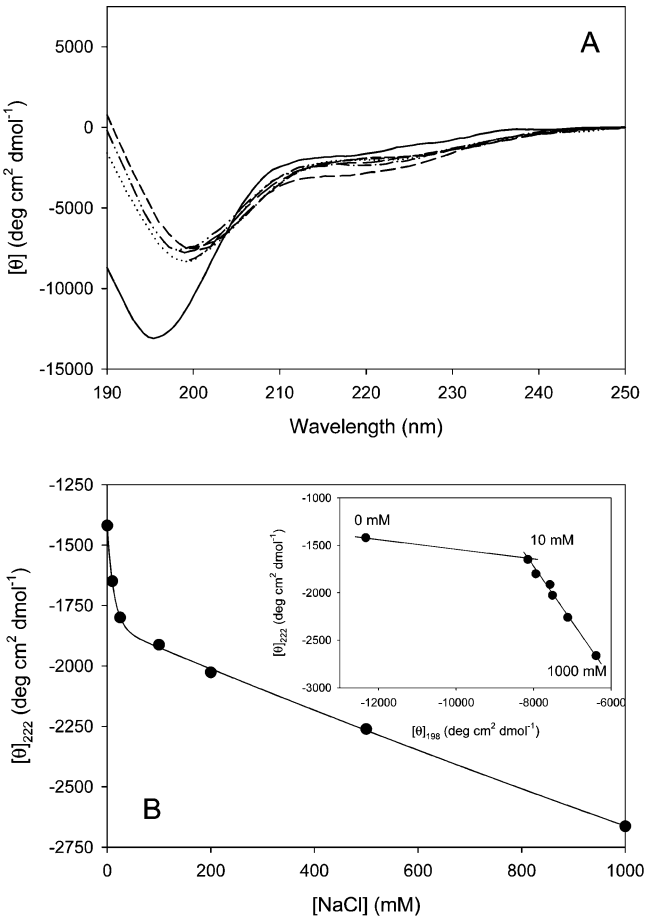

FIGURE 1: NaCl-induced conformational changes in α-synuclein. (A) Far-UV CD spectra of 35 μM α-synuclein as a function of NaCl concentration: 0, 10, 25, 100, 200, 500, and 1000 mM (in order of the increasingly negative $[\theta]_{222}$ value; see panel B). The cell path length was 0.1 mm. Measurements were carried out at 20 °C and pH 7.4. (B) Effect of NaCl on $[\theta]_{222}$ of human α-synuclein. (Inset) Phase diagram ($[\theta]_{222}$ versus $[\theta]_{198}$) illustrating the NaCl-induced structure formation in α-synuclein. NaCl concentration values are indicated in the vicinity of the corresponding symbol.

to that reported earlier for the amyloidogenic partially folded intermediate of α-synuclein (*9*). Thus, NaCl induces partial folding of this natively unfolded protein.

Figure 1B represents the dependence of $[\theta]_{222}$ on NaCl concentration and shows that the salt-induced folding of α-synuclein is a biphasic transition, with major changes taking place at low salt concentrations. The inset to Figure 1B, where the results are plotted in the form of a "phase diagram" (parametric dependence), confirms this, revealing that the first transition occurs between 0 and 10 mM and the second above 10 mM NaCl (typical intracellular concentration is about 10 mM NaCl). The parametric dependence approach suggests that the dependence of $[\theta]_{\lambda_1}$ vs $[\theta]_{\lambda_2}$ will be linear if changes in the protein environment lead to all-or-none transitions between two different conformations (*23*, *28*−*32*). On the other hand, nonlinearity of this function reflects multiple sequential transformations. Each linear portion of such a plot describes an individual all-or-none transition. The inset to Figure 1B shows that the phase diagram consists of two linear parts, reflecting the existence of at least two independent transitions induced in α-synuclein by NaCl. The structural changes observed by CD were completely reversible (data not shown) and were independent

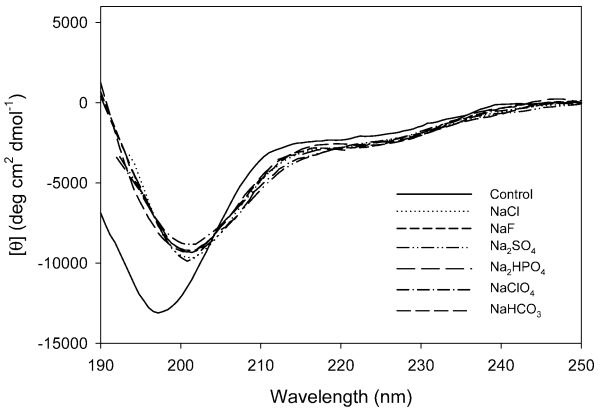

FIGURE 2: Anion-induced conformational changes in α-synuclein. Far-UV circular dichroism spectra of 35 μM α-synuclein measured in the absence or in the presence of 200 mM of the following anions: control (solid line), chloride (dotted), fluoride (dashed), sulfate (dash-double dot), phosphate (long dash), perchlorate (dash−dot), and carbonate (medium dash). The cell path length was 0.1 mm. Measurements were carried out at 20 °C and pH 7.5.

of protein concentration (at least in the range of 0.1−2.5 mg/mL; data not shown). This indicates that the increase in structure of α-synuclein induced by NaCl is an intramolecular process and does not involve self-association.

Effect of Different Anions on the Secondary Structure of α*-Synuclein.* Figure 2 compares the effects of 200 mM concentrations of different anions—Cl^-, F^-, SO_4^{2-}, HPO_4^{2-}, HCO_3^-, and ClO_4^-—on the far-UV CD spectra of human α-synuclein. All the anions were in the form of their sodium salts. Each of the anions studied induced a comparable degree of folding in α-synuclein at this concentration. The CD spectra of α-synuclein in the presence of these different anions were similar to the spectrum of the amyloidogenic partially folded intermediate of α-synuclein (*9*).

Effect of Anions on the Fibrillation of α*-Synuclein at Neutral pH.* Thioflavin T is a fluorescent dye that interacts preferentially with amyloid fibrils, leading to a characteristic increase in the fluorescence intensity in the vicinity of 480 nm (*34*). When α-synuclein solutions were incubated under conditions leading to fibrils, the fluorescence of ThT at 482 nm followed a characteristic sigmoidal curve, i.e., an initial lag phase, a subsequent growth phase, and a final equilibrium phase, as seen in Figure 3A. Such curves are consistent with a nucleation-dependent elongation model of protein fibrillation, in which the three phases (lag, exponential increase, and final leveling off) correspond to nucleation, extension, and equilibrium phases.

Effect of Increasing Chloride Concentration on α*-Synuclein Fibrillation.* Figure 3A shows the effects of different NaCl concentrations on the kinetics of α-synuclein fibrillation. Fibril formation for the anion-free α-synuclein was a very slow process (lagtime of 34 h, and elongation rate of 0.06 h^{-1}), whereas the kinetics of fibril formation increased dramatically in the presence of salt (e.g., at 500 mM the lagtime was 6 h and the elongation rate 0.4 h^{-1}). Figure 3B compares the effect of the increasing salt concentration on the kinetic parameters of α-synuclein fibrillation. The increase in NaCl concentration was accompanied by a considerable reduction of the lag time and a substantial increase in the rate of fibril growth. The inset to Figure 3B shows a plot of the dependence of elongation rate on

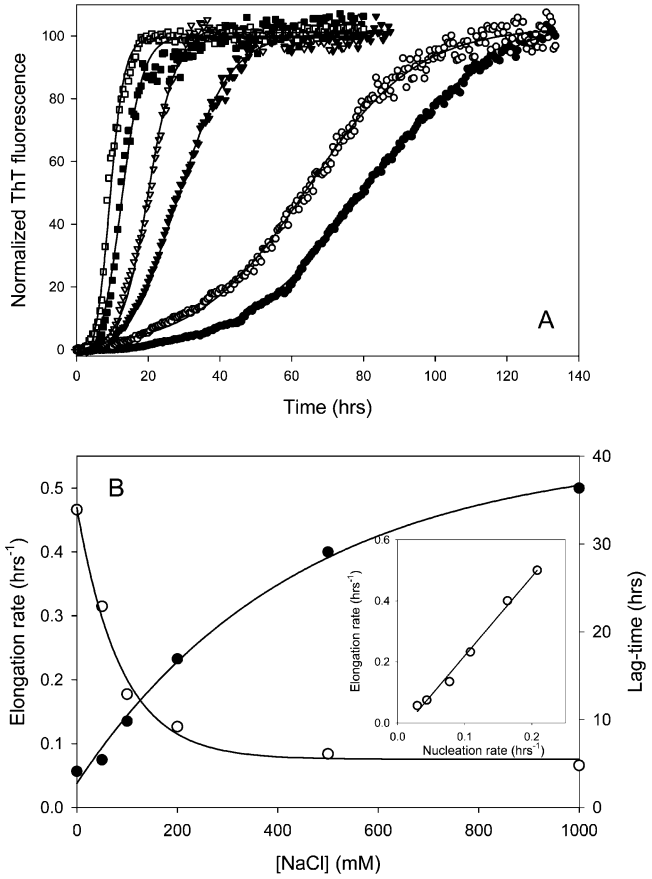

FIGURE 3: Effect of NaCl on the fibrillation of human α-synuclein at neutral pH. (A) Kinetics of α-synuclein fibrillation at different NaCl concentrations monitored by changes in ThT fluorescence. The symbols represent ThT fluorescence intensities determined experimentally, and the lines are fitted according to ref *33*. NaCl concentrations were 0 (●), 50 (○), 100 (▼), 200 (▽), 500 (■), and 1000 mM (□). Protein concentration was 35 μM. Measurements were carried out at 37 °C with agitation. (B) Dependence of elongation rate (●) and lag time (○) of α-synuclein fibrillation on NaCl concentration. (Inset) Elongation rate versus nucleation rate (1/lag time) for the fibrillation of α-synuclein in the presence of different concentrations of NaCl.

nucleation rate (calculated as 1/lag time). The linear relationship shows that the rates of the two key processes of α-synuclein fibrillation, nucleation and elongation, were both affected in a similar manner by increasing salt concentration.

Different Anions Accelerate Fibrillation of α*-Synuclein to a Different Extent.* To compare the effect of different anions, we analyzed the fibrillation of human α-synuclein in the presence of 200 mM concentrations of the following salts: NaF, NaCl, NaBr, NaN_3, $NaNO_3$, Na_2SO_4, $NaClO_4$, $Na_2S_2O_3$, Na_2HPO_4, $NaHCO_3$, HCOONa, CH_3COONa, and CCl_3COONa. The results of these experiments are summarized in Figure 4A, and Table 1. There are several important observations to note: (i) all anions studied accelerate the fibrillation of α-synuclein; (ii) the effectiveness of acceleration depends on the nature of anions; and (iii) anions affect nucleation and elongation of α-synuclein fibrillation in a similar way—i.e., shorter lag-time, faster fibril growth. This last conclusion is illustrated by Figure 4B, which compares fibril elongation and nucleation (inverse lag time) rates for α-synuclein fibrillation in the presence of the different anions. Interestingly, an excellent correlation exists between the ability of a given anion to accelerate the nucleation of fibrils

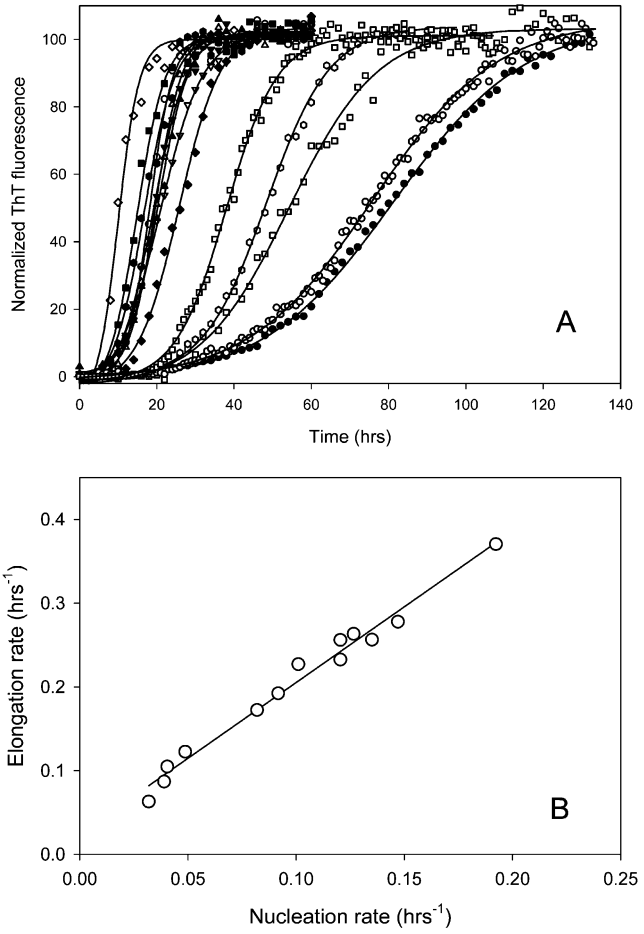

FIGURE 4: Effect of different anions on the fibrillation of α-synuclein at neutral pH. (A) Kinetics of α-synuclein fibrillation in the presence of 200 mM concentrations of different anions monitored by changes in ThT fluorescence. The symbols represent ThT fluorescence intensities determined experimentally, and the lines are fitted according to ref *33*. The sodium salts of mono- and divalent anions were used: control, no salt (black circles), N_3^- (gray circles), HCO_3^- (open squares), ClO_4^- (open hexagons), $S_2O_3^{2-}$ (gray squares), NO_3^- (black diamonds), Br^- (open reversed triangles), Cl^- (black inverse triangles), $HCOO^-$ (black triangles), CH_3COO^- (open triangles), CCl_3COO^- (black hexagons), F^- (open circles), HPO_4^{2-} (black squares), and SO_4^{2-} (open diamonds). The anions are listed according to the increasing capability to promote fibrillation. Protein concentration was kept at 35 μM. Measurements were carried out at 37 °C with agitation. (B) Dependence of the elongation rate on the nucleation rate of α-synuclein fibrillation in the presence of various anions (200 mM) at neutral pH. The anions are ordered according to the increasing ability to accelerate the fibrillation: N_3^-, HCO_3^-, ClO_4^-, $S_2O_3^{2-}$, NO_3^-, Br^-, CH_3COO^-, Cl^-, $HCOO^-$, F^-, CCl_3COO^-, HPO_4^-, and SO_4^{2-}.

and to promote fibril elongation. Figure 4B shows that the effectiveness of the anions in increasing the rate of fibrillation at neutral pH follows the series

$$N_3^- < HCO_3^- < ClO_4^- < S_2O_3^{2-} < NO_3^- < Br^- < Cl^- < HCOO^- \approx CH_3COO^- < CCl_3COO^- \approx F^- < HPO_4^{2-} < SO_4^{2-} \quad (1)$$

Effect of Increasing Concentrations of Various Anions on the Kinetics of Fibrillation of α*-Synuclein.* We next compared the effect of increasing concentration of the different anions on the rate of α-synuclein fibrillation (Figure 5). Anions from the above series (1) could be divided in two

Table 1: Kinetic Parameters of α-Synuclein Fibrillation in the Presence of Different Anions (200 mM) at pH 7.4[a]

salt	$t_{1/2}$ (h)	lag time (h)	(elongation rate)$^{-1}$ (h)
none	69.3 ± 0.4	33.9 ± 0.2	17.7 ± 0.2
Na_2SO_4	10.6 ± 0.2	5.2 ± 0.1	2.7 ± 0.1
Na_2HPO_4	14.0 ± 0.2	6.8 ± 0.1	3.6 ± 0.1
CCl_3COONa	15.2 ± 0.3	7.4 ± 0.2	3.9 ± 0.1
NaF	15.5 ± 0.3	7.9 ± 0.2	3.8 ± 0.1
HCOONa	14.7 ± 0.3	8.3 ± 0.2	3.2 ± 0.1
NaCl	16.9 ± 0.3	8.3 ± 0.2	4.3 ± 0.1
CH_3COONa	17.4 ± 0.3	9.0 ± 0.2	4.2 ± 0.1
NaBr	21.3 ± 0.3	10.9 ± 0.3	5.2 ± 0.1
$NaNO_3$	23.8 ± 0.4	12.2 ± 0.3	5.8 ± 0.2
$Na_2S_2O_3$	35.7 ± 0.4	19.5 ± 0.3	8.1 ± 0.2
$NaClO_4$	41.1 ± 0.4	22.7 ± 0.3	9.2 ± 0.2
$NaHCO_3$	48.6 ± 0.4	25.6 ± 0.3	11.5 ± 0.2
NaN_3	63.1 ± 0.4	31.3 ± 0.3	15.9 ± 0.2

[a] Data from analysis of Figure 4.

groups according to their concentration effects on α-synuclein aggregation. Anions from the middle and the end of the series, $HCOO^-$, CH_3COO^-, and $S_2O_4^{2-}$, formed one group, in which an increase in anion concentration led to a proportional increase in the rate of α-synuclein nucleation and elongation (Figure 5A, B, and C, respectively). On the other hand, anions from the beginning of the series, $S_2O_3^{2-}$, ClO_4^-, and NO_3^-, formed a separate group, in which the effect of the anion concentration did not lead to proportional effects on the rate of fibrillation (Figure 5D−F). For example, low concentrations of these latter three anions (in the range from 50 to 200 mM) showed little variation in their effects on the rate of fibrillation. Furthermore, for ClO_4^- (Figure 5E) and NO_3^- (Figure 5F), the accelerating effect of 50 mM anion was somewhat more pronounced than the effect of 100 mM. These effects likely arise from a combination of specific anion binding to the protein and compensating effects from the cations and anions on the net interaction of the ions with the protein.

Morphology of α-Synuclein Fibrils Grown in the Presence of Different Anions. Fibril formation was further analyzed by electron microscopy (EM). EM analysis was used to study the morphology of the aggregated material induced by incubation of α-synuclein in the presence of the different anions. As illustrated in Figure 6, for a representative selection of anions, there was no significant difference in the overall morphology of fibrils grown in the absence or in the presence of different anions.

Effect of Anions on α-Synuclein Fibrillation at Acidic pH. The fibrillation of human α-synuclein is substantially accelerated at low pH (*9*). We analyzed the effect of various anions (200 mM concentrations of NaCl, NaBr, $NaNO_3$, $NaClO_4$, NaH_2PO_4, $Na_2S_2O_3$, and Na_2SO_4) on the kinetics of fibril formation at low pH (pH 2.0). Figure 7A represents the results of this analysis and shows that the fibrillation of α-synuclein at acidic pH was significantly faster than that at neutral pH. Furthermore, as at neutral pH, the anions accelerated both the rates of nucleation and elongation of α-synuclein fibrillation in a correlated manner at acidic pH (Figure 7B). No corrections were made for the low pH effect on anion concentration for SO_4^{2-} ($pK_a = 1.9$) and $S_2O_3^{2-}$ ($pK_a = 1.72$) that will be significantly protonated at pH 2.0.

Although the kinetics of fibril formation were still dependent on the nature of the anion at low pH, the order of effectiveness was dramatically different from that observed at neutral pH. In fact, the anions which were the least effective at neutral pH became the most effective at low pH (Figure 7B, Table 2), namely

$$Cl^- < Br^- \approx H_2PO_4^- < NO_3^- < SO_4^{2-} < S_2O_3^{2-} < ClO_4^- \quad (2)$$

The data in Figure 8 provide additional support to the conclusion that a decrease in pH reverses the order of the effectiveness of different anions in accelerating fibrillation. The relative increases in anion-induced rates of fibrillation are shown as $V_{acid}/V_{neutral}$ ratios, where V_{acid} and $V_{neutral}$ correspond to nucleation (or elongation) rates measured for the given anion at acidic and neutral pH, respectively. Figure 8 shows that the largest changes in the effects of the anions in accelerating α-synuclein fibrillation are for the anions NO_3^-, $S_2O_3^{2-}$, and ClO_4^-.

Combined Effect of Cations and Anions on the Fibrillation of α-Synuclein. We also analyzed how different cations affect the kinetics of α-synuclein fibrillation induced by different anions. To this end, the kinetics of α-synuclein fibrillation were compared in the presence of increasing concentrations of different salts: NH_4NO_3, NH_4Cl, $(NH_4)_2SO_4$, $Mg(NO_3)_2$, $MgCl_2$, and $MgSO_4$ (Figure 9). The results show that NH_4^+ salts accelerate fibrillation of α-synuclein in a concentration-dependent manner, with larger salt concentrations giving a larger accelerating effect. Furthermore, Figure 9A−C shows that, analogous to the sodium salts, different ammonium salts accelerate α-synuclein fibrillation to a different extent, following the series

$$(NH_4)_2SO_4 > NH_4NO_3 > NH_4Cl \quad (3)$$

Interestingly, the effect of different Mg^{2+} salts was more dramatic, leading to a very short lag time and relative independence on concentration (at least in the concentration range studied), and did not vary much with the nature of the anions (see Figure 9D,E). The series describing the fibril-promoting effect of different Mg^{2+} salts is as follows:

$$MgSO_4 \geq Mg(NO_3)_2 \approx MgCl_2 \quad (4)$$

The kinetic data are summarized in Figure 10, which compares the kinetic parameters of α-synuclein fibrillation measured at the different concentrations of different salts. The salts were grouped according to the nature of their anions. Clearly, cations possess a more potent effect on the elongation rate of α-synuclein fibrillation, whereas nucleation is somewhat less dependent on the nature of the cation (cf. Figure 10A−C and 10D,E).

DISCUSSION

α-Synuclein belongs to the family of natively unfolded or intrinsically unstructured proteins (*9*, *35*, *36*), which are characterized by a lack of ordered structure under physiological conditions in vitro (*37*−*43*). This absence of folded structure has been attributed to the specific combination of low overall hydrophobicity and large net charge (*38*, *40*, *41*). Analysis of the amino acid sequence shows that α-synuclein is highly charged at physiological pH. In fact, at pH 7.5, it has 24 negatively charged side chains and 15 positively

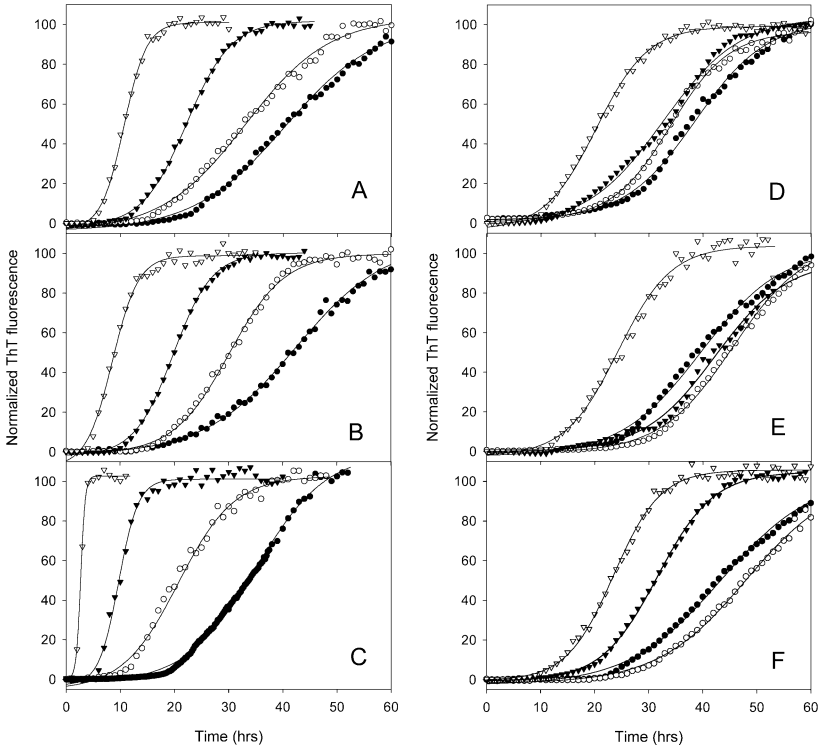

FIGURE 5: Concentration dependence of the effect of different anions in accelerating the fibrillation of α-synuclein. The reactions were monitored by changes in ThT fluorescence: $HCOO^-$ (A), CH_3COO^- (B), SO_4^{2-} (C), $S_2O_3^{2-}$ (D), ClO_4^- (E), and NO_3^- (F). Salts concentrations were 50 (●), 100 (○), 200 (▼), and 500 mM (▽).

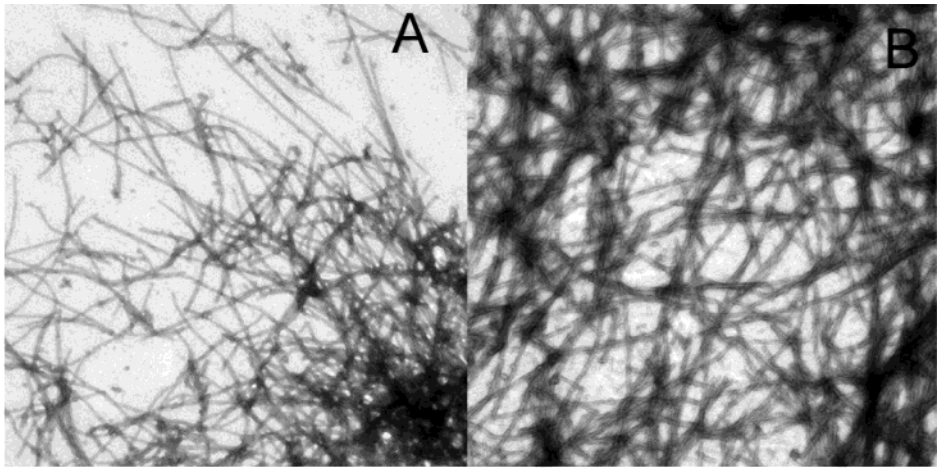

FIGURE 6: Fibril morphology is independent of anions in α-synuclein fibrillation. Negative stained transmission electron micrographs of α-synuclein fibrils prepared in the presence of 200 mM of (A) chloride and (B) nitrate.

charged side chains (the net charge is −9), with the majority of negatively charged side chains being localized within the C-terminal domain of the protein (Figure 11). Thus, α-synuclein is natively unfolded, mainly because of the electrostatic repulsion between the net negative charges. To some extent this resembles the situation occurring for many globular proteins at low or high pH. It is well documented that unfolded proteins under conditions of extreme pH can be transformed into more compact, structured conformations when the net electrostatic repulsion is reduced by the binding of oppositely charged ions (*44*−*48*). We have previously shown that α-synuclein is partially folded at neutral pH in the presence of a variety of mono-, di-, and trivalent metal ions. In fact, the structure-forming effectiveness of cations directly correlated with their increasing charge density. This metal ion-stimulated partial folding of intrinsically unstructured α-synuclein, which occurs at micromolar to low millimolar cation concentration, was attributed to the effective neutralization of the Coulombic repulsion between negative charges. For polyvalent cations, an additional important factor, the potential for cross-linking or bridging between two or more carboxylates, was proposed (*20*). A strong correlation was observed between the effectiveness of metal ions to induce a conformational change and their efficiencies to stimulate fibrillation of α-synuclein (*20*), consistent with the cation-induced conformation being the critical amyloidogenic intermediate structure.

α-Synuclein has also been shown to bind specifically to several unstructured polycations, including spermine, polyethylenimine, poly-L-lysine, and poly-L-arginine. This interaction led to the oligomerization of α-synuclein and significantly accelerated the rate of α-synuclein fibrillation. The

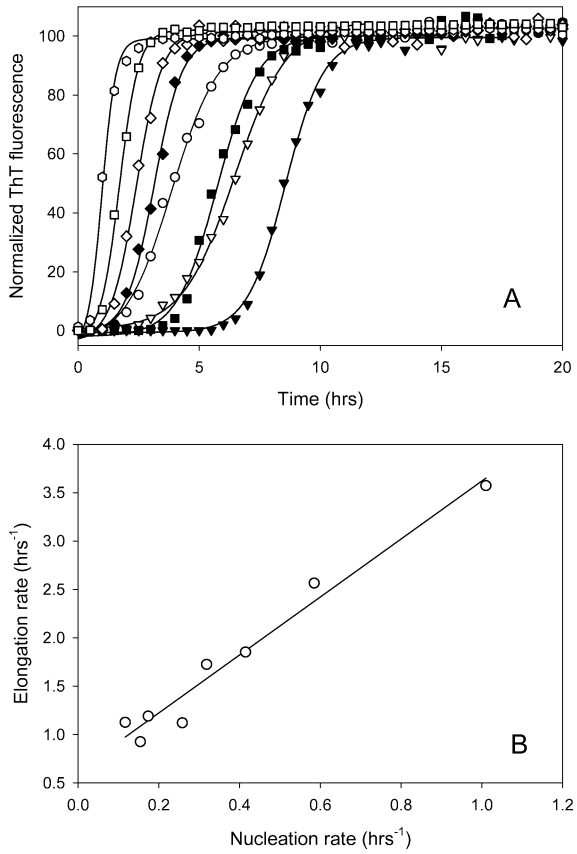

FIGURE 7: Effect of various anions on α-synuclein fibrillation at acidic pH. (A) Kinetics of α-synuclein fibrillation in the presence of 200 mM concentrations of different anions monitored by changes in ThT fluorescence. The symbols represent ThT fluorescence intensities determined experimentally, and the lines are fitted according to ref *33*. The sodium salts of mono- and divalent anions were used: Cl^- (black inverse triangles), Br^- (open inverse triangles), $H_2PO_4^-$ (black squares), NO_3^- (black diamonds), SO_4^{2-} (open diamonds), $S_2O_3^{2-}$ (gray squares), and ClO_4^- (open hexagons). The anions are listed according to their increasing capability to promote fibrillation. Protein concentration was kept at 35 μM. Measurements were carried out at 37 °C with agitation. (B) Dependence of the elongation rate on the nucleation rate of α-synuclein fibrillation in the presence of various anions at pH 2.0 (kinetic parameters determined from curve-fitting; see Methods section). The anions are ordered according to the increasing ability to accelerate the fibrillation of human α-synuclein: Cl^-, Br^-, $H_2PO_4^-$, SO_4^{2-}, NO_3^-, $S_2O_3^{2-}$, and ClO_4^-.

Table 2: Kinetic Parameters of α-Synuclein Fibrillation in the Presence of Different Anions (200 mM) at pH 2.0[a]

salt	$t_{1/2}$ (h)	lag time (h)	(elongation rate)$^{-1}$ (h)
$NaClO_4$	0.99 ± 0.01	0.43 ± 0.01	0.28 ± 0.02
$Na_2S_2O_3$	1.71 ± 0.02	0.93 ± 0.01	0.39 ± 0.02
Na_2SO_4	2.41 ± 0.03	1.33 ± 0.02	0.54 ± 0.03
$NaNO_3$	3.14 ± 0.03	1.98 ± 0.02	0.58 ± 0.03
NaH_2PO_4	5.76 ± 0.03	4.08 ± 0.03	0.84 ± 0.03
NaBr	6.48 ± 0.03	4.32 ± 0.03	1.08 ± 0.04
NaCl	8.56 ± 0.04	6.98 ± 0.04	0.79 ± 0.04

[a] Data from analysis of Figure 7.

magnitude of the accelerating effect depended on the chemical nature of the polycation, its length, and its concentration (*21*). It has been suggested that polycations accelerate α-synuclein fibrillation by minimizing the electrostatic repulsion between negatively charged α-synuclein molecules, resulting in a localized high concentration of α-synuclein, favoring fibrillation (*21*).

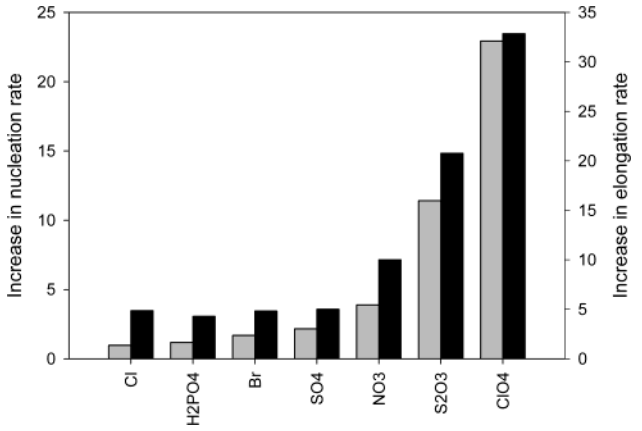

FIGURE 8: Effect of pH on the nucleation and elongation rates of α-synuclein fibrillation in the presence of various anions. Increases in rates were calculated as $V_{acid}/V_{neutral}$ ratio, where V_{acid} and $V_{neutral}$ represent nucleation (gray bars) [or elongation (black bars)] rates measured at pH 2 and 7, respectively.

Interestingly, anionic GAGs have also been shown to accelerate α-synuclein fibrillation (*18*). Binding sites on a variety of proteins for heparin invariably contain clusters of basic amino acid residues capable of binding to the negatively charged heparin polymer (*49*). The N-terminal region of α-synuclein contains clusters of positive charge from its repeats of the consensus sequence KTKEGV (see Figure 11). GAGs may preferentially bind to the amyloidogenic conformation of α-synuclein, or the binding of GAG may result in a highly localized α-synuclein concentration that favors fibrillation (since the GAGs are incorporated in, or associated with, the fibrils) (*18*).

The results presented here show that, in addition to cations, polycations, and polyanions, different anions also can dramatically affect the rate of fibrillation of human α-synuclein. In the first part of the investigation, similar molar concentrations of different sodium salts (200 mM) were used, so we can exclude the contribution of the cation and focus on the effect of the anions. The fibrillation of α-synuclein starts with formation of the amyloidogenic partially folded intermediate (*9*) and follows a nucleation−polymerization mechanism (*11*). The circular dichroism data established that, at a concentration of 200 mM, all the salts studied induced comparable partial folding of α-synuclein. In contrast, the fibrillation kinetics profiles were dramatically different in the presence of different anions. This means that different anions differentially affect the nucleation and/or elongation stages of the fibrillation process. An additional noteworthy point is that conformational effects of the anions could be broken down into two effects. Low concentrations of anion (<10 mM) led to significant change in ellipticity, whereas subsequent increases in anion concentration had much smaller effects on the ellipticity and secondary structure. This suggests two different types of effects of the anions, as discussed subsequently. The fact that anions increased both the rates of nucleation and fibril growth suggest a common underlying phenomenon. The circular dichroism spectrum of the partially folded intermediate indicates that there is little helix in the intermediate. Association most likely occurs via the N-terminal region, especially the NAC region (residues 62−91), which has several positively charged lysine residues.

What is the mechanism of the fibrillation-modulating effect of anions? The effects of salts on protein structure and

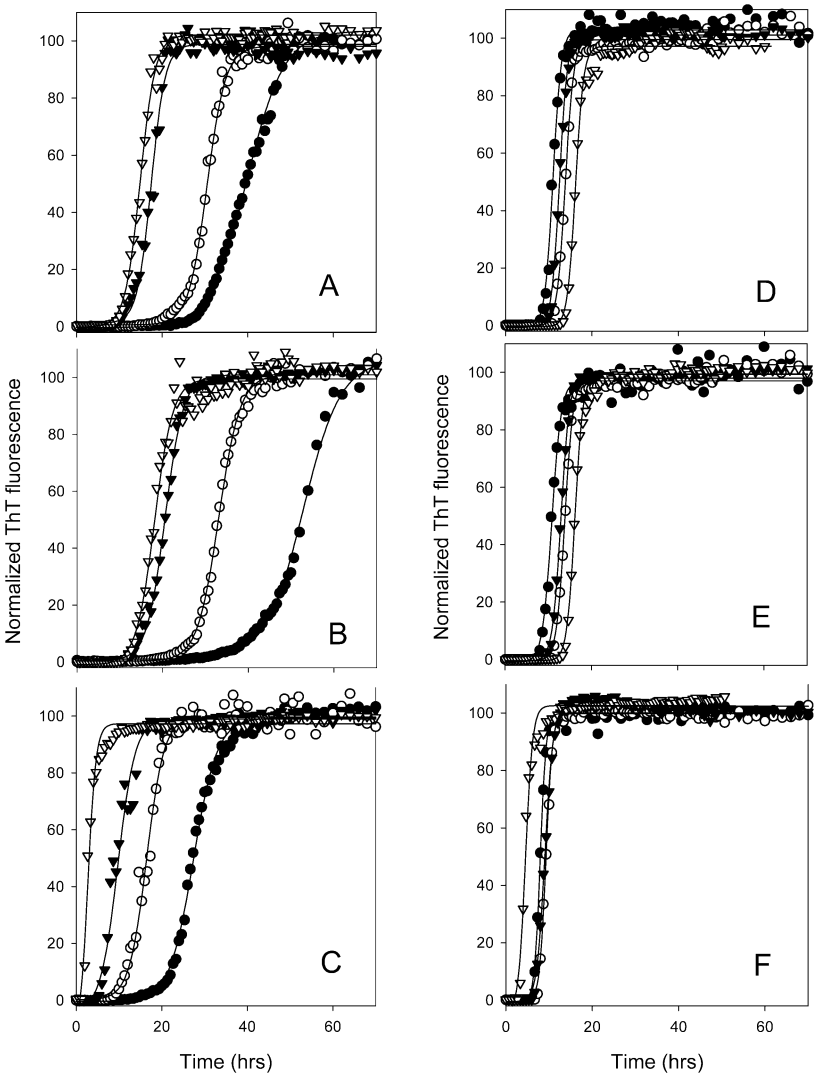

FIGURE 9: Cation−anion pair effects on the fibrillation of α-synuclein at neutral pH. Kinetics of α-synuclein fibrillation in the presence of increasing concentrations of different salts monitored by changes in ThT fluorescence: (A) NH_4NO_3, (B) NH_4Cl, (C) $(NH_4)_2SO_4$, (D) $Mg(NO_3)_2$, (E) $MgCl_2$, and (F) $MgSO_4$. Salt concentrations were 50 (●), 100 (○), 200 (▼), and 500 mM (▽). The symbols represent ThT fluorescence intensities determined experimentally, and the lines are fitted according to ref *33*. Protein concentration was kept at 35 μM. Measurements were carried out at 37 °C with agitation.

association are complex and may be specific or nonspecific; e.g., salts may bind directly to various side chains in the protein or may interact with solvent water. In addition to the electrostatic effects, anions interact with the solvent water and can affect both the water−water and protein−water interactions, leading to an increase or decrease in the hydrophobic interactions of proteins. Generally, the effects of low salt concentration are due mostly to neutralization of the net charge on the protein, whereas the effects of high salt concentrations are determined by the net effect of the three competing preferential interactions (between water, protein, and salt ions). Several different models have been proposed to account for the effects of salts on aqueous solutions of proteins.

The association of α-synuclein will involve both hydrophobic and electrostatic interactions between side chains, as well as changes in hydration. Figure 11 shows that 11 of 15 positive charges are localized within the N-terminal half of α-synuclein. They represent potential sources of the Coulombic charge−charge repulsion, contributing to the intrinsically disordered nature of the protein, as well as to the intermolecular electrostatic repulsion between the protein molecules. Anions can reduce this repulsion either by the Debye−Hückel screening effect or by direct interaction with positive charges via specific ion-pair formation, i.e., specific anion binding. If the Debye−Hückel screening has the major contribution, then the effect of various anions will be determined by the ionic strength of the solution. Since similar concentrations were used for all the salts (200 mM), the calculated ionic strength was 200 and ∼600 mM for the solutions of mono- and divalent anions, respectively. The majority of the anions were monovalent (i.e., their solutions have similar ionic strength) but showed significant variation in their effects on the kinetics of fibrillation (see Table 1 and Figure 12A). The same was also true for the divalent anions. Here, SO_4^{2-} and HPO_4^{2-} induced the fastest fibrillation, whereas $S_2O_3^{2-}$ was among the least effective (Table 1, Figure 12A). Thus, we conclude that the major effect of the anions in modulating the rate of α-synuclein fibrillation is not due to Debye−Hückel screening.

The importance of direct anion binding to fibrillation can be determined by comparing the effectiveness of various

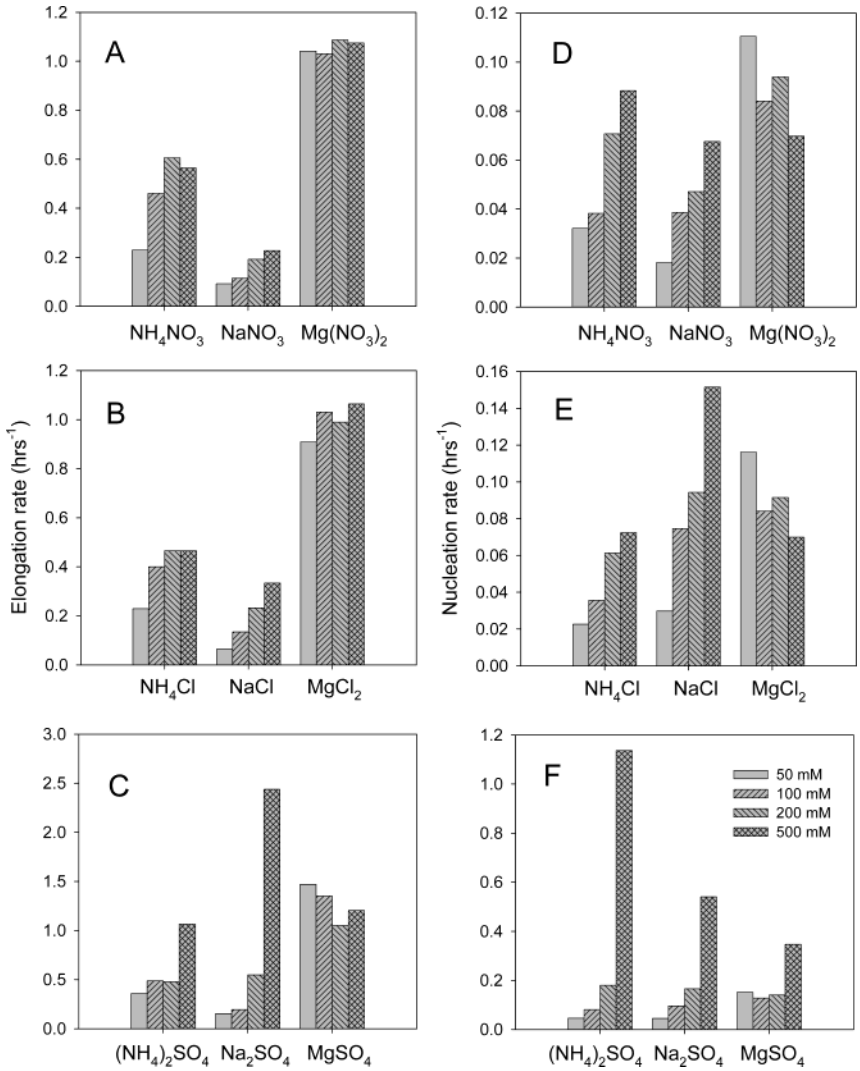

FIGURE 10: Cation−anion pair effects on the kinetic parameters of α-synuclein fibrillation at neutral pH. The elongation rates (A−C) and nucleation rates (D−F) are plotted as a function of increasing concentration of different salts. Data are grouped according to the nature of the anion: (A and D) NH_4NO_3, $NaNO_3$, and $Mg(NO_3)_2$; (B and E) NH_4Cl, NaCl, and $MgCl_2$; (C and F) $(NH_4)_2SO_4$, Na_2SO_4, and $MgSO_4$.

anions with the electroselectivity series of the anions toward anion-exchange resins (*50*, *51*). According to this electroselectivity series, anions can be arranged in the following order (from weaker to stronger binders to the anion-exchange resin Amberlite XAD-1) (*51*):

$$F^- < CH_3COO^- < HCOO^- < H_2PO_4^- < HCO_3^- < Cl^- < NO_2^- < Br^- < NO_3^- < I^- < SCN^- < ClO_4^- < SO_4^{2-} < SO_3^{2-} < C_2O_4^{2-} < CrO_4^{2-} < S_2O_3^{2-} \quad (5)$$

Figure 12B shows the general lack of correlation between the efficiency of a given anion to accelerate fibrillation of α-synuclein and its position within the electroselectivity series. Hence, we conclude that specific anion binding does not play a significant role in determining the effect of anions on fibrillation at higher anion concentrations (>10 mM).

The effects at high salt concentrations indicate that salt-induced folding and aggregation arose from alteration in the protein−water interaction. If water−anion interactions are important for the modulation of α-synuclein fibrillation, then the fibril-promoting effectiveness of various anions should follow the Hofmeister series (known also as the lyotropic series) (*52*). The Hofmeister series for the anions, in descending order of their salting-out effectiveness, was as follows (*53*):

$$\text{citrate} > \text{tartrate} > SO_4^{2-} > Cl^- > NO_3^- > ClO_4^- > I^- > SCN^- \quad (6)$$

Currently it is widely recognized that the Hofmeister series is critical to an understanding of water−solute interactions (*54*). In fact, the salting-out effect may be compared to the relative influence of the ions on other physicochemical processes, such as changes in the surface tension of water (*55*), denaturation of biological macromolecules, including proteins (*56*), and salt-induced activation of lyophilized enzymes (*57*). It is known that the Hofmeister series effect plays an important role in the modulation of protein crystallization (*58*); the crystallization of proteins is more affected by anions than by cations. Furthermore, it has been shown that the ability of anions to induce crystallization of proteins follows the Hofmeister series if the protein is crystallized at a pH above the p*I*. However, when a protein is crystallized at a pH below its p*I*, the effect of anions as

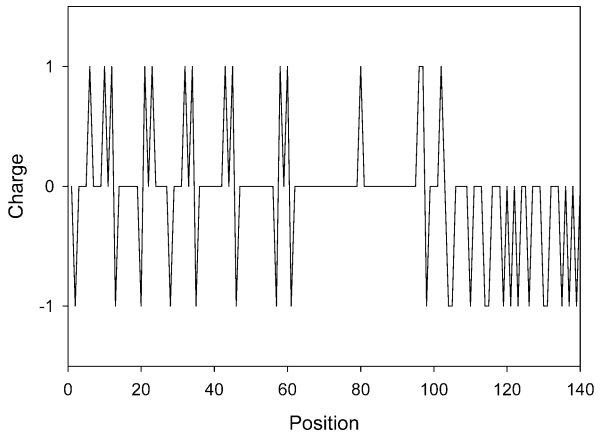

FIGURE 11: Distribution of positive and negative charges in the α-synuclein sequence.

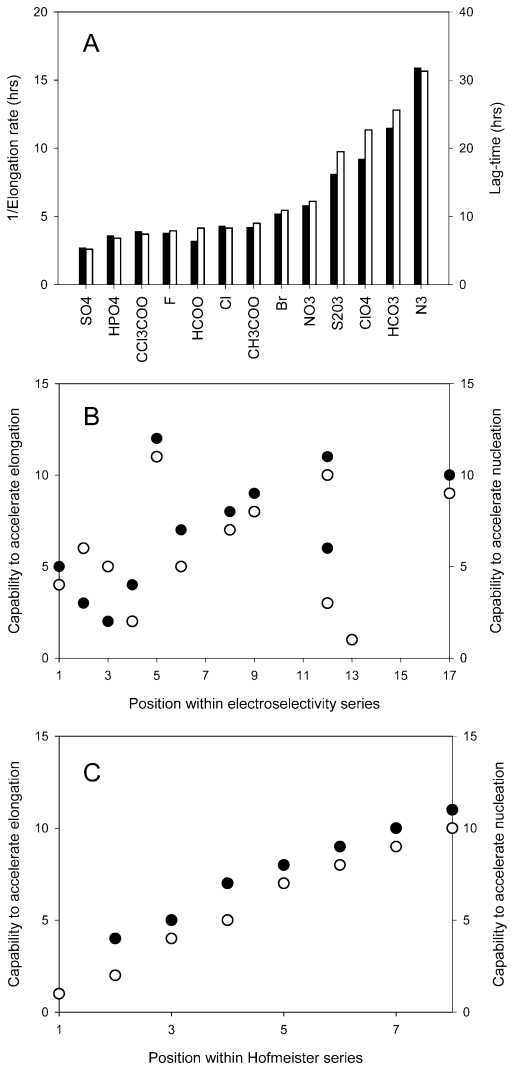

FIGURE 12: Correlations between anion properties and α-synuclein fibrillation rates. (A) Kinetic parameters of α-synuclein fibrillation, 1/elongation rate (black symbols), and lag time (open symbols) determined for different anions (as their sodium salts) at neutral pH (From Figure 4). Correlation of the anion effect on rates of elongation (black symbols) and nucleation (open symbols) with different properties of anions: position of anion within the electroselectivity series (B), and position within the Hofmeister series (C).

the crystallizing agents follows the reverse order of the Hofmeister series (*58*−*61*). Thus, the effectiveness of anions in inducing protein crystallization may be reversed depending on the net charge of the protein, i.e., depending on whether the protein is crystallized at a pH above or below its isoelectric point. The mechanism that leads to inversion of the Hofmeister series is unknown as yet. However, this phenomenon may be a general one, as the order of anions and cations in the Hofmeister series for ovalbumin coagulation was reversed if the protein solutions were acidified (*62*).

In the present investigation, we have established that the anions are arranged in the following order with respect to their effectiveness in stimulating α-synuclein fibril formation at neutral pH (see Table 1, Figures 4A and 12A):

$$SO_4^{2-} > HPO_4^{2-} > F^- \approx CCl_3COO^- > CH_3COO^- \approx HCOO^- > Cl^- > Br^- > NO_3^- > S_2O_3^{2-} \gg HCO_3^- > ClO_4^- > N_3^- \quad (7)$$

This series generally follows the Hofmeister series of the anions (Figure 12C) (*54*):

$$SO_4^{2-} > HPO_4^{2-} > F^- > Cl^- > Br^- > NO_3^- > S_2O_3^{2-} > ClO_4^- > SCN^- \quad (8)$$

Furthermore, the order of anions in our series was reversed when α-synuclein fibrillation was studied at a pH below its p*I* of 4.67, as observed in salting-out and crystallization. It is likely that the observed reversal of the anion effect on fibrillation at low pH reflects binding of anions to neutralize excess positive charge. In the majority of cases, the positions of ions in the Hofmeister series correspond to the degree of their hydration (*63*); i.e., small ions of high charge density bind water tightly, whereas large monovalent ions of low charge density bind water weakly (relative to water−water interaction strength): this is seen in the Jones−Dole viscosity *B* coefficients (*64*). However, the relative position should be considered as indicative only, because there will be considerable variation with protein, pH, and temperature. Furthermore, the relative order of cations may reverse with different anions (e.g., NO_3^- rather than Cl^-) under some circumstances due to ion pair effects (*65*). In agreement with this conclusion, we observed that, when ammonium salts were used, nitrate accelerated fibrillation of α-synuclein more effectively than chloride (see Figures 9 and 10). It is likely that the ions bind to α-synuclein at neutral pH loosely and nonspecifically, assuming that α-synuclein can be treated as a polyelectrolyte; i.e., the ions condense around the protein to neutralize the charge. This is consistent with our observations that the nature of the charge-screening cation was less important than the nature of the anion. As expected, we observed that kosmotropes (such as sulfate) are more effective than chaotropes in inducing folding and aggregation. It is also possible that collapse of different portions of α-synuclein affect fibrillation, depending on the nature of the ions present. For example, Na^+ might be most effective at causing a "simple collapse" of the C-terminus, weakly hydrated anions might cause collapse of the N-terminal domain, divalent Mg^{2+} might cause more complex conformational effects by "cross-linking" or bridging multiple carboxylates, and sulfate might be most effective at collapsing the whole molecule.

Our data are consistent with the conclusion that moderate concentrations of anions modulate the nucleation and elongation stages of α-synuclein fibrillation primarily via their effect on changes in the interactions of water (Hofmeister series effect). From this perspective, fibrillation could be considered a particular case of the more general phenomenon of protein salting-out. Nevertheless, the degree to which anions interact with water, stabilizing the hydrophobic interactions within the α-synuclein molecule or between protein molecules, is not the only factor determining the stability and solubility of this protein, and electrostatic effects have to be taken into account as well.

Consequently, the enhanced fibrillation of α-synuclein in the presence of anions is the result of the loss of the uncompensated charge, which is a factor promoting the soluble unfolded conformation, and an increase in the preferential hydration, which promotes partial folding and aggregation by strengthening hydrophobic interactions. Both key steps of fibrillation, nucleation and fibril growth, are affected by a combination of these two effects. The addition of the first small quantities of salts eliminates the strong repulsion due to the net electrical charges, giving rise to partial folding of α-synuclein (Figure 1), whereas the continued addition of the salt brings about dehydration that results ultimately in fibrillation of the protein. Since cations bind more tightly to α-synuclein (*19*), it is possible that the structural transition observed in Figure 1 reflects initial collapse of the C-terminal domain (negatively charged), followed by subsequent collapse of the N-terminal domain (positively charged). However, this is unlikely, since the C-terminus is predicted to have no propensity for ordered secondary structure.

Our conclusion is therefore that anions promote fibrillation of α-synuclein through a combination of electrostatic and solvent (hydration) effects. It is reasonable to assume that these factors, especially the latter, will apply to the fibrillation of other proteins, especially those that are relatively unstructured. In addition, our conclusions suggest that the underlying basis for the effects of many other endogenous and exogenous factors on fibrillation will involve their interactions with water.

REFERENCES

1. Lewy, F. H. (1912) in *Handbuch der Neurologie* (Lewandowski, M., Ed.) pp 920−933, Springer, Berlin.
2. Forno, L. S. (1996) Neuropathology of Parkinson's disease, *J. Neuropathol. Exp. Neurol. 55*, 259−272.
3. Maroteaux, L., Campanelli, J. T., and Scheller, R. H. (1988) Synuclein: a neuron-specific protein localized to the nucleus and presynaptic nerve terminal, *J. Neurosci. 8*, 2804−2815.
4. Jakes, R., Spillantini, M. G., and Goedert, M. (1994) Identification of two distinct synucleins from human brain, *FEBS Lett. 345*, 27−32.
5. Iwai, A., Masliah, E., Yoshimoto, M., Ge, N., Flanagan, L., de Silva, H. A., Kittel, A., and Saitoh, T. (1995) The precursor protein of non-A beta component of Alzheimer's disease amyloid is a presynaptic protein of the central nervous system, *Neuron 14*, 467−475.
6. George, J. M., Jin, H., Woods, W. S., and Clayton, D. F. (1995) Characterization of a novel protein regulated during the critical period for song learning in the zebra finch, *Neuron 15*, 361−372.
7. George, J. M. (2002) The synucleins, *Genome Biol. 3*, REVIEWS3002.1−3002.6.
8. Uversky, V. N., and Fink, A. L. (2002) Amino acid determinants of alpha-synuclein aggregation: putting together pieces of the puzzle, *FEBS Lett. 522*, 9−13.
9. Uversky, V. N., Li, J., and Fink, A. L. (2001) Evidence for a partially folded intermediate in alpha-synuclein fibril formation, *J. Biol. Chem. 276*, 10737−10744.
10. Crowther, R. A., Jakes, R., Spillantini, M. G., and Goedert, M. (1998) Synthetic filaments assembled from C-terminally truncated *a*-synuclein, *FEBS Lett. 436*, 309−312.
11. Wood, S. J., Wypych, J., Steavenson, S., Louis, J. C., Citron, M., and Biere, A. L. (1999) alpha-synuclein fibrillogenesis is nucleation-dependent. Implications for the pathogenesis of Parkinson's disease, *J. Biol. Chem. 274*, 19509−19512.
12. Giasson, B. I., Uryu, K., Trojanowski, J. Q., and Lee, V. M. (1999) Mutant and wild-type human alpha-synucleins assemble into elongated filaments with distinct morphologies in vitro, *J. Biol. Chem. 274*, 7619−7622.
13. Narhi, L., Wood, S. J., Steavenson, S., Jiang, Y., Wu, G. M., Anafi, D., Kaufman, S. A., Martin, F., Sitney, K., Denis, P., Louis, J. C., Wypych, J., Biere, A. L., and Citron, M. (1999) Both familial Parkinson's disease mutations accelerate alpha-synuclein aggregation, *J. Biol. Chem. 274*, 9843−9846.
14. Serpell, L. C., Berriman, J., Jakes, R., Goedert, M., and Crowther, R. A. (2000) Fiber diffraction of synthetic alpha-synuclein filaments shows amyloid-like cross-beta conformation, *Proc. Natl. Acad. Sci. U.S.A 97*, 4897−4902.
15. Conway, K. A., Harper, J. D., and Lansbury, P. T., Jr. (2000) Fibrils formed in vitro from alpha-synuclein and two mutant forms linked to Parkinson's disease are typical amyloid, *Biochemistry 39*, 2552−2563.
16. Li, J., Uversky, V. N., and Fink, A. L. (2001) Effect of familial Parkinson's disease point mutations A30P and A53T on the structural properties, aggregation, and fibrillation of human alpha-synuclein, *Biochemistry 40*, 11604−11613.
17. Hoyer, W., Antony, T., Cherny, D., Heim, G., Jovin, T. M., and Subramaniam, V. (2002) Dependence of alpha-synuclein aggregate morphology on solution conditions, *J. Mol. Biol. 322*, 383−393.
18. Cohlberg, J. A., Li, J., Uversky, V. N., and Fink, A. L. (2002) Heparin and other glycosaminoglycans stimulate the formation of amyloid fibrils from alpha-synuclein in vitro, *Biochemistry 41*, 1502−1511.
19. Uversky, V. N., Li, J., and Fink, A. L. (2001) Metal-triggered structural transformations, aggregation, and fibrillation of human alpha-synuclein−A possible molecular link between Parkinson's disease and heavy metal exposure, *J. Biol. Chem. 276*, 44284−44296.
20. Uversky, V. N., Li, J., Bower, K., and Fink, A. L. (2002) Synergistic effects of pesticides and metals on the fibrillation of α-synuclein: Implications for Parkinson's disease, *Neurotoxicology 23*, 527−536.
21. Goers, J., Uversky, V. N., and Fink, A. L. (2003) Polycation-induced oligomerization and accelerated fibrillation of human alpha-synuclein in vitro, *Protein Sci. 12*, 702−707.
22. Uversky, V. N., Li, J., and Fink, A. L. (2001) Trimethylamine-N-oxide-induced folding of alpha-synuclein, *FEBS Lett. 509*, 31−35.
23. Munishkina, L. A., Phelan, C., Uversky, V. N., and Fink, A. L. (2003) Conformational behavior and aggregation of alpha-synuclein in organic solvents: Modeling the effects of membranes, *Biochemistry 42*, 2720−2730.
24. Manning-Bog, A. B., McCormack, A. L., Li, J., Uversky, V. N., Fink, A. L., and Di Monte, D. A. (2002) The herbicide paraquat causes up-regulation and aggregation of alpha-synuclein in mice: paraquat and alpha-synuclein, *J. Biol. Chem. 277*, 1641−1644.
25. Uversky, V. N., Li, J., and Fink, A. L. (2001) Pesticides directly accelerate the rate of alpha-synuclein fibril formation: a possible factor in Parkinson's disease, *FEBS Lett. 500*, 105−108.
26. Goers, J., Manning-Bog, A. B., McCormack, A., Millett, I. S., Doniach, S., Dimonte, D. A., Uversky, V. N., and Fink, A. L. (2003) Nuclear localization of a-synuclein and its interaction with histones, *Biochemistry 42*, 8465−8471.
27. Uversky, V. N., Yamin, G., Souillac, P. O., Goers, J., Glaser, C. B., and Fink, A. L. (2002) Methionine oxidation inhibits fibrillation of human alpha-synuclein in vitro, *Febs Lett. 517*, 239−244.
28. Burstein, E. A. (1976) *Intrinsic Protein Fluorescence: Origin and Applications*, VINIITI, Moscow.
29. Permyakov, E. A., Yarmolenko, V. V., Emelyanenko, V. I., Burstein, E. A., Closset, J., and Gerday, C. (1980) Fluorescence

Studies of the Calcium-Binding to Whiting (Gadus-Merlangus) Parvalbumin, *Eur. J. Biochem. 109*, 307−315.
30. Bushmarina, N. A., Kuznetsova, I. M., Biktashev, A. G., Turoverov, K. K., and Uversky, V. N. (2001) Partially folded conformations in the folding pathway of bovine carbonic anhydrase II: A fluorescence spectroscopic analysis, *ChemBioChem 2*, 813−821.
31. Kuznetsova, I. M., Stepanenko, O. V., Turoverov, K. K., Zhu, L., Zhou, J. M., Fink, A. L., and Uversky, V. N. (2002) Unraveling multistate unfolding of rabbit muscle creatine kinase, *Biochim. Biophys. Acta 1596*, 138−155.
32. Turoverov, K. K., Kuznetsova, I. M., and Uversky, V. N. (2002) in *Recent Research Developments in Biophysics* (Pandalai, S. G., Ed.) pp 101−119, Transworld Research Network, Kerala, India.
33. Nielsen, L., Khurana, R., Coats, A., Frokjaer, S., Brange, J., Vyas, S., Uversky, V. N., and Fink, A. L. (2001) Effect of environmental factors on the kinetics of insulin fibril formation: Elucidation of the molecular mechanism, *Biochemistry 40*, 6036−6046.
34. Naiki, H., Higuchi, K., Matsushima, K., Shimada, A., Chen, W. H., Hosokawa, M., and Takeda, T. (1990) Fluorometric examination of tissue amyloid fibrils in murine senile amyloidosis: use of the fluorescent indicator, thioflavine T, *Lab. Invest. 62*, 768−773.
35. Weinreb, P. H., Zhen, W., Poon, A. W., Conway, K. A., and Lansbury, P. T., Jr. (1996) NACP, a protein implicated in Alzheimer's disease and learning, is natively unfolded, *Biochemistry 35*, 13709−13715.
36. Uversky, V. N. (2003) A protein-chameleon: Conformational plasticity of a-synuclein, a disordered protein involved in neurodegenerative disorders, *J. Biomol. Struct. Dyn. 21*, 211−234.
37. Wright, P. E., and Dyson, H. J. (1999) Intrinsically unstructured proteins: re-assessing the protein structure−function paradigm, *J. Mol. Biol. 293*, 321−331.
38. Uversky, V. N., Gillespie, J. R., and Fink, A. L. (2000) Why are "natively unfolded" proteins unstructured under physiologic conditions? *Proteins 41*, 415−427.
39. Dunker, A. K., Lawson, J. D., Brown, C. J., Williams, R. M., Romero, P., Oh, J. S., Oldfield, C. J., Campen, A. M., Ratliff, C. M., Hipps, K. W., Ausio, J., Nissen, M. S., Reeves, R., Kang, C., Kissinger, C. R., Bailey, R. W., Griswold, M. D., Chiu, W., Garner, E. C., and Obradovic, Z. (2001) Intrinsically disordered protein, *J. Mol. Graph. Model. 19*, 26−59.
40. Uversky, V. N. (2002) Natively unfolded proteins: a point where biology waits for physics, *Protein Sci. 11*, 739−756.
41. Uversky, V. N. (2002) What does it mean to be natively unfolded? *Eur. J. Biochem. 269*, 2−12.
42. Tompa, P. (2002) Intrinsically unstructured proteins. *Trends Biochem. Sci. 27*, 527−533.
43. Uversky, V. N. (2003) Protein folding revisited. A polypeptide chain at the folding−misfolding−nonfolding cross-roads: which way to go? *Cell Mol. Life Sci. 60*, 1852−1871.
44. Goto, Y., and Fink, A. L. (1989) Conformational states of beta-lactamase: molten-globule states at acidic and alkaline pH with high salt, *Biochemistry 28*, 945−952.
45. Goto, Y., Calciano, L. J., and Fink, A. L. (1990) Acid-induced folding of proteins, *Proc. Natl. Acad. Sci. U.S.A. 87*, 573−577.
46. Goto, Y., Takahashi, N., and Fink, A. L. (1990) Mechanism of acid-induced folding of proteins, *Biochemistry 29*, 3480−3488.
47. Fink, A. L., Calciano, L. J., Goto, Y., Kurotsu, T., and Palleros, D. R. (1994) Classification of acid denaturation of proteins−intermediates and unfolded states, *Biochemistry 33*, 12504−12511.
48. Uversky, V. N., Karnoup, A. S., Segel, D. J., Seshadri, S., Doniach, S., and Fink, A. L. (1998) Anion-induced folding of Staphylococcal nuclease: characterization of multiple equilibrium partially folded intermediates, *J. Mol. Biol. 278*, 879−894.
49. Cardin, A. D., and Weintraub, H. J. R. (1989) Molecular Modeling of Protein−Glycosaminoglycan Interactions, *Arteriosclerosis 9*, 21−32.
50. Gregor, H. P., Belle, J., and Marcus, R. A. (1955) Studies on Ion-exchange Resins. XIII. Selectivity Coefficients of Quaternary Base Anion-exchange Resins Toward Univalent Anions, *J. Am. Chem. Soc. 77*, 2713−2719.
51. Gjerde, D. T., Schmuckler, G., and Fritz, J. S. (1980) Anion Chromatography with Low-Conductivity Eluents. 2, *J. Chromatogr. 187*, 35−45.
52. Hofmeister, F. (1888) On the understanding of the effects of salts. On regularities in the precipitating effect of salts and their relationship to their physiological behavior, *Arch. Exp. Pathol. Pharmakol. (Leipzig) 24*, 247−260.
53. McBain, J. W. (1950) *Colloid Science*, D. C. Heath and Co., Boston, New York, Chicago, Atlanta, San Francisco, Dallas, London.
54. Collins, K. D., and Washabaugh, M. W. (1985) The Hofmeister effect and the behaviour of water at interfaces, *Q. Rev. Biophys. 18*, 323−422.
55. Hartman, R. J. (1939) *Colloid Chemistry*, Houghton Mifflin Co., The Riverside Press Cambridge, Boston, New York, Chicago, Dallas, Atlanta, San Francisco.
56. Baldwin, R. L. (1996) How Hofmeister Ion Interactions Affect Protein Stability, *Biophys. J. 71*, 2056−2063.
57. Ru, M. T., Hirokane, S. Y., Lo, A. S., Dordick, J. S., Reimer, J. A., and Clark, D. S. (2000) On the salt-induced activation of lyophilized enzymes in organic solvents: Effect of salt kosmotropicity on enzyme activity, *J. Am. Chem. Soc. 122*, 1565−1571.
58. Tardieu, A., Finet, S., and Bonnete, F. (2001) Structure of the macromolecular solutions that generate crystals, *J. Crystal Growth 232*, 1−9.
59. Tardieu, A., Le Verge, A., Malfois, M., Bonnete, F., Finet, S., Ries-Kautt, M., and Belloni, L. (1999) Proteins in solution: from X-ray scattering intensities to interaction potentials, *J. Crystal Growth 196*, 193−203.
60. Rieskautt, M. M., and Ducruix, A. F. (1989) Relative Effectiveness of Various Ions on the Solubility and Crystal-Growth of Lysozyme. *J. Biol. Chem. 264*, 745−748.
61. Carbonnaux, C., Rieskautt, M., and Ducruix, A. (1995) Relative Effectiveness of Various Anions on the Solubility of Acidic Hypoderma-Lineatum Collagenase at Ph 7.2, *Protein Sci. 4*, 2123−2128.
62. Thomas, A. W. (1934) *Colloid Chemistry*, McGraw-Hill Book Co., Inc., New York, London.
63. Zavitsas, A. A. (2001) Properties of water solutions of electrolytes and nonelectrolytes, *J. Phys. Chem. B 105*, 7805−7817.
64. Collins, K. D. (1995) Sticky ions in biological systems, *Proc. Natl. Acad. Sci. U.S.A. 92*, 5553−5557.
65. Lo Nostro, P., Fratoni, L. U., Ninham, B. W., and Baglioni, P. (2002) Water absorbency by wool fibers: Hofmeister effect. *Biomacromolecules 3*, 1217−1224.

BI034938R